Vietnam Journal of Catalysis and Adsorption
Tạp chí xúc tác và hấp phụ Việt Nam

http://jca.edu.vn

Removal of Fe^{3+} ions from polluted water using heat-pretreated and H_3PO_4 modified oyster shells

Truong Ngoc Tuan[1], Luong Doanh Chinh[2], Le Huynh Nhi[3], Nguyen Thi Hong Phuong[2], Nguyen Ba Cuong[3], Vu Minh Chau[4], Nguyen Thi Hoai Phuong[4,*]

[1] *Institute of Technology, Vietnam Defence Industry, 3 Van Hoi, Dong Ngac, Hanoi, Vietnam*
[2] *School of Chemistry and Life Sciences, Hanoi University of Science and Technology, 1 Dai Co Viet, Hanoi, Vietnam*
[3] *Faculty of Physics and Chemistry Engineering, Military Technical Academy, 236 Hoang Quoc Viet, Ha Noi, Vietnam*
[4] *Department of Chemistry and Environment, Joint Vietnam-Russia Tropical Science and Technology Research Center, 63 Nguyen Van Huyen, Hanoi, Vietnam*
** Email: hoaiphuong.vrtc@gmail.com*

ARTICLE INFO

Received: 19/07/2025
Accepted: 25/09/2025
Published: 30/09/2025

Keywords:
Modified oyster shell;
Fe^{3+} removal;
adsorption kinetics;
isotherm models;
wastewater treatment

ABSTRACT

Oyster shells pretreated by calcination at 500 °C and chemically modified with H_3PO_4 were used in this study to enhance surface reactivity for efficient removal of Fe^{3+} ions from polluted water. Characterization by SEM, XRD, and FTIR confirmed significant structural and chemical changes, including the formation of phosphate-containing compounds. Batch adsorption experiments revealed that modified oyster shells exhibited high Fe^{3+} removal efficiency, achieving near-complete removal (~100%) within 120 minutes. Kinetic modeling indicated that the adsorption process followed pseudo-second-order and Bangham models, suggesting chemisorption and intraparticle diffusion as dominant mechanisms. Isotherm analysis showed the best fit with Sips and Redlich–Peterson models, reflecting heterogeneous surface adsorption behavior. The removal of Fe^{3+} ions effectiveness of modified oyster shells as a low-cost, sustainable, and eco-friendly adsorbent for Fe^{3+} remediation, providing a promising approach to heavy metal pollution.

Introduction

The contamination of water resources by heavy metal ions poses a significant environmental and public health challenge worldwide. Among various heavy metals, ferric ions (Fe^{3+}) are commonly found in industrial effluents, particularly from mining, steel manufacturing, and metal finishing industries [1]. Elevated concentrations of Fe^{3+} in water can lead to severe ecological consequences, including the disruption of aquatic ecosystems, and posing health risks to humans through consuming contaminated water [2]. Therefore, removing Fe^{3+} ions from polluted water is critical for environmental sustainability and public safety. Conventional methods, including chemical precipitation [3], ion exchange [4], membrane filtration [5], and adsorption [6], each approach have their advantages and limitations for removing heavy metal ions from water. Among these ways, adsorption has gained considerable attention due to its simplicity, cost-

https://doi.org/10.62239/jca.2025.032

effectiveness, and high efficiency for removing low concentrations of metal ions. The choice of adsorbent material is a key factor that determines the success of the adsorption process. Recently, there has been a growing interest in utilizing waste-derived and low-cost natural materials as adsorbents, to reduce treatment costs and to promote resource recycling [7,8].

Oyster shells, a byproduct of the seafood industry, are generated in large quantities and often pose disposal challenges. Composed primarily of calcium carbonate ($CaCO_3$), oyster shells have demonstrated potential as adsorbent materials for various pollutants [9,10]. However, their native adsorption capacity is often limited due to low surface area and a lack of active binding sites [11]. To enhance their efficiency, physical and chemical modifications have been explored. Heat treatment increases porousity and increase their surface area, while chemical modification introduces functional groups that enhance metal ion binding [12,13].

This study investigates the removal of Fe^{3+} ions from polluted water using oyster shells that have been both heat-pretreated and modified with H_3PO_4. The combined modification approach aims to maximize the adsorption capacity of oyster shells by enhancing their structural and chemical properties. The main goals of this research are to (1) examine how heat and H_3PO_4 treatment change the physical and chemical properties of oyster shells, (2) test how well Fe^{3+} can be removed under different concentrations and contact times, and (3) study how the adsorption process works. By valorizing an abundant waste material, this study not only proposes an effective solution for Fe^{3+} remediation but also contributes to sustainable waste management practices.

Experimental

Chemical

Phosphoric acid (H_3PO_4, 85%) and Iron(III) chloride hexahydrate ($FeCl_3{\cdot}6H_2O$, 99%) were sourced from Xilong, China. Discarded oyster shells, collected from Pacific oysters in the Van Don area of Quang Ninh province, Vietnam, were used for the study.

Preparation of modified oyster shells

The raw oyster shells were cleaned, dried at room temperature (Fig 1a), then calcined at 500 °C for 2 h to obtain raw oyster shells (ROS) [14]. The calcined material was ground and sieved (<0.22 µm), then phosphatized by reacting 10 g of shells with 75 mL of 0.5 mol L^{-1} H_3PO_4 at 65 °C for 2 h. The solids were washed to neutral pH and dried at 90 °C for 4 h, yielding modified oyster shells (MOS-Fig 1b).

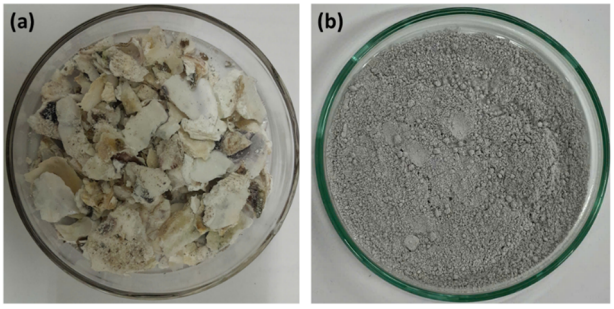

Fig 1: Cleaned raw oyster shell pieces (a) and heat- and H_3PO_4-modified oyster shell powder (b).

Characterization

Oyster shell morphology was observed by SEM (Hitachi S-4800). Phase composition was analyzed by XRD (X'Pert Pro, CuKα, 10°–70° 2θ), and functional groups were identified by FTIR (TENSOR II, 4000–400 cm^{-1}).

Adsorption properties

A 250 ppm Fe^{3+} stock solution was prepared from $FeCl_3{\cdot}6H_2O$. For adsorption, 0.1 g of sample was mixed with 100 mL of Fe^{3+} solution, stirred at 200 rpm at room temperature, then filtered for Fe analysis by ICP-MS (Agilent 7700x, Japan). The applied kinetic models include the pseudo-first-order, pseudo-second-order, Elovich, Bangham, and intraparticle diffusion models [15]. In adsorption isotherm experiment, Fe^{3+} solutions (50–300 ppm) were treated with 0.1 g of adsorbent in 100 mL, stirred at 160 rpm for 24 h at room temperature, and the data were fitted to Langmuir, Temkin, Redlich–Peterson, Sips, and Toth isotherm models [16].

The pseudo-first-order model: $q_t = q_1(1 - e^{k_1 t})$

The pseudo-second-order model: $q_t = \frac{t}{\frac{1}{k_2 q_2^2} + \frac{t}{q_2}}$

The Elovich model: $q_t = \frac{1}{\beta}\ln(1 + \alpha\beta t)$

The Bangham model: $q_t = k_B \times t^{a_B}$

The intraparticle diffusion model: $q_t = k_I t^{0.5} + C$

where k_1 (min^{-1}), k_2 (g mg^{-1} min^{-1}), k_B (mg g^{-1} $s^{-\alpha}$), and K_I (mg g^{-1} $min^{-0,5}$) constantly correspond to the models. α, β is the correlation parameter in the Elovich model. q_t (mg g^{-1}) is the adsorption capacity at the time t (min). The parameter a_B of Bangham indicates the adsorption intensity. C is a constant related to the thickness of the fluid film surrounding the adsorbent.

Langmuir model: $q_e = \frac{K_L Q_m C_e}{1 + K_L C_e}$;

Temkin model: $q_e = b_T ln A C_e$

Redlich-Peterson (R-P) model: $q_e = \frac{Q_m K_R C_e}{(1 + (K_R C_e)^n)^{\frac{1}{n}}}$

https://doi.org/10.62239/jca.2025.032

Toth model: $q_e = \frac{Q_m K_T C_e}{(1+(K_T C_e)^n)^{\frac{1}{n}}}$

where C_e (mg L^{-1}) is the Fe^{3+} concentration at equilibrium (mg L^{-1}), q_e is the adsorption capacity at equilibrium q_{max} (mg g^{-1}) is the maximum adsorption capacity of oyster shell K_L (L g^{-1}), and K_R (L g^{-1}) are the representative constants of the Langmuir, and Redlich-Peterson models constant, respectively. n is a parameter related to the surface heterogeneity. b_T (kJ mol^{-1}) is the Temkin constant related to the heat of adsorption. R (kJ mol^{-1} K^{-1}) is the gas constant, and T is the absolute temperature (K).

Results and discussion

Characterization of modified oyster shell

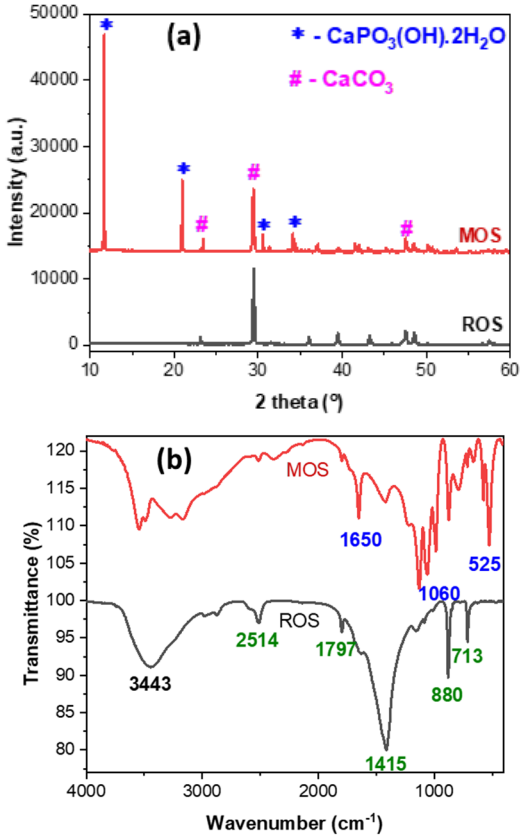

Fig 1: XRD pattern (a) and FTIR spectra (b) of raw oyster shell pieces (black) and modified oyster shell (red)

The XRD patterns in Fig 2a reveal clear differences between ROS (black) and MOS (red). The ROS sample exhibits distinct diffraction peaks corresponding to crystalline $CaCO_3$ (calcite) at 2θ ≈ 23.0°, 29.4°, and 47.5°, consistent with standard calcite structures (PDF 00-005-0586) [17]. After modification with H_3PO_4, the MOS sample shows reduced intensity of these $CaCO_3$ peaks and the emergence of new peaks at 2θ ≈ 12.0°, 21.0°, 31.5°, and 34.0°, which are assigned to $CaPO_3(OH)·2H_2O$ (PDF 00-009-0077), indicating successful chemical transformation [17]. The decreased crystallinity of $CaCO_3$ and the appearance of calcium phosphate hydrate phases confirm that phosphoric acid reacted with $CaCO_3$, partially converting it into phosphate species. This structural change likely enhances surface reactivity and contributes to improved adsorption performance. Thus, the XRD results strongly support the effective chemical modification of ROS into a more functional material (MOS) with mixed-phase composition.

The FTIR spectra of ROS (black) is depicted in Fig 2b. The black portion of the spectrum displays significant absorption bands at approximately 1415 cm^{-1} and 880 cm^{-1}. These bands correspond to the asymmetric and out-of-plane bending vibrations of carbonate (CO_3^{2-}) groups in calcite. O–H stretching and bending at around 3443 cm^{-1} and a faint signal near 1650 cm^{-1} are attributed to the presence of adsorbed water, which causes the broadband signal. MOS (red) exhibits a decrease in the strength of the carbonate bands, while the appearance of additional bands occurs around ~1060 cm^{-1}. This indicates the presence of P–O stretching vibrations that are associated with phosphate groups. The inclusion of phosphate species into the structure has been successfully accomplished, as demonstrated by these results. Both the chemical alteration and surface functionalization of ROS are supported by the changes in FTIR characteristics, which ultimately result in the formation of MOS.

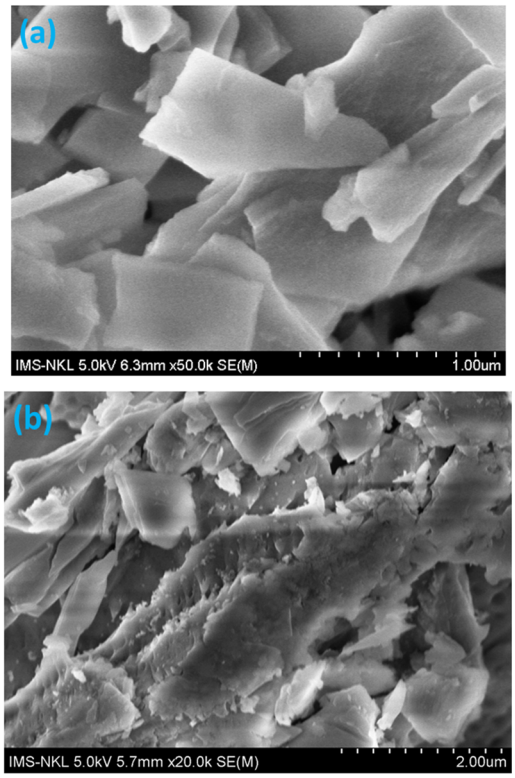

Fig 2: SEM images of raw oyster shell pieces (a) and modified oyster shell (b).

https://doi.org/10.62239/jca.2025.032

The SEM image of the raw oyster shell (ROS, Fig. 3a) shows a mostly smooth and thick layered structure made up of stacked flat pieces, which is typical of crystalline calcium carbonate ($CaCO_3$). The surfaces appear clean with minimal porosity, reflecting a compact mineral structure. In contrast, the SEM image of modified oyster shell (MOS, Fig. 3b) displays significant morphological transformation. The surface becomes rougher and more irregular, with etched features, cracks, and increased surface texture. These changes indicate that some of the $CaCO_3$ structure has dissolved and new materials, probably in the form of calcium phosphate, have formed, which matches what the XRD results show. The rough texture and uneven structure show that the surface has been successfully changed, which should improve how well the material can attract and react with other substances. The SEM observations show that treating with phosphoric acid treatment alters the ROS's surface structure, which could create larger surface area and active sites that are good for environmental uses.

Kinetics of Fe^{3+} adsorption on modified oyster shell

The kinetic behavior of Fe^{3+} adsorption onto MOS was evaluated using five models: pseudo-first order, pseudo-second order, Elovich, Bangham, and intraparticle diffusion.

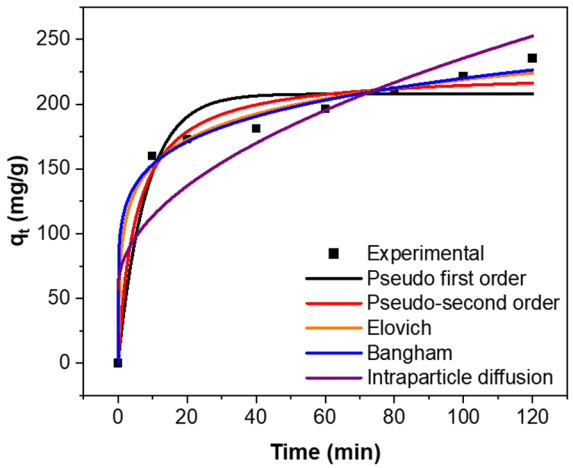

Fig 3: Kinetics of Fe^{3+} adsorption model on modified oyster shell.

As shown in Fig 4 and Table 1, the experimental data (black squares) fit best with the pseudo-second order (red line) and Bangham (blue line) models, with R^2 values of 0.972 and 0.993, respectively. These high coefficients of determination suggest that chemisorption and pore diffusion are the dominant mechanisms. Pseudo-second order model: The best fitting among the conventional models, with a high adjusted R^2 of 0.972 and a calculated equilibrium adsorption capacity (q_e) of 225.783 mg/g. This conclusion suggests that electron sharing or exchange between Fe and active sites on MOS controls the adsorption process. Bangham model: Shows the highest adjusted R^2 (0.993) and the lowest reduced χ^2 value (45.15), indicating a strong match with how particles move through pores. The result indicates that Fe^{3+} ions likely penetrate internal pores after initial surface binding. Elovich model: This model also works well (R^2 = 0.990), showing that the surface where adsorption happens is uneven and that the process involves chemical bonding with different energy levels, which is typical for modified natural materials like MOS. Pseudo-first order model: Shows a lower R^2 (0.943) and deviation from experimental data, indicating it does not adequately describe the system. Intraparticle diffusion model: With an R^2 of 0.808, this model does not solely govern the process but suggests it plays a secondary role alongside surface interaction.

Fe^{3+} adsorption onto MOS occurs primarily through chemisorption and also involves some movement through pores, following specific patterns known as pseudo-second order and Bangham kinetics. These results show that MOS could be a good material for removing Fe^{3+} from water. Taken together, the kinetic fitting and structural characterization suggest a dual mechanism in which chemisorption dominates the initial binding of Fe^{3+} onto surface functional groups, followed by intraparticle diffusion into the porous matrix of the modified oyster shell.

Table 1: Parameter Kinetics of Fe^{3+} adsorption model on modified oyster shell.

Model	Parameter	Value
Pseudo-first order	k_1 (min^{-1})	0.123
	q_e ($mg.g^{-1}$)	207.967
	R^2	0.943
Pseudo-second order	k_2 ($g.mg^{-1}.min^{-1}$)	$8.426.10^{-4}$
	q_e ($mg.g^{-1}$)	225.783
	R^2	0.972
Elovich	α ($mg.g^{-1}$)	571.645
	β ($g.mg^{-1}$)	0.035
	R^2	0.990
Bangham	a_B	0.157
	k_B	106.818
	χ^2	45.15
	R^2	0.993
Intrapartical diffusion	K_I ($mg.g^{-1}.min^{-0.5}$)	17.862
	q_t ($mg.g^{-1}$)	56.970
	R^2	0.808

https://doi.org/10.62239/jca.2025.032

The adsorption isotherm of Fe^{3+} on modified oyster shell (MOS) demonstrates a typical pattern of rapid uptake at low equilibrium concentrations (C_e), followed by gradual saturation, indicating high initial affinity and eventual site exhaustion. Among the models tested, the Redlich–Peterson isotherm matched the experimental data the best across all concentration levels, which means that adsorption happens on a surface that has different types of binding strengths. At elevated concentrations, the Langmuir, Temkin, and Toth models demonstrate moderate concordance yet differ. The results suggest that Fe^{3+} adsorption on MOS involves complicated processes beyond just a single layer of adsorption, likely including ion exchange, surface complex formation, and interactions with different active sites.

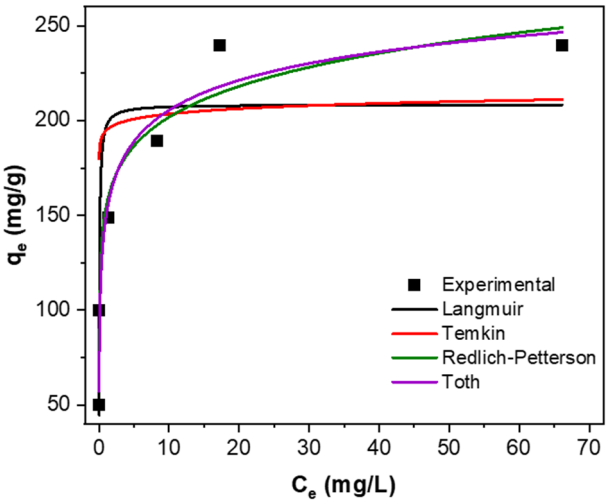

Fig. 4: Isotherm adsorption model of Fe^{3+} on modified oyster shell.

Table 2: Parameter of Isotherm adsorption model of Fe^{3+} on modified oyster shell.

Model	Parameter	Value
Langmuir	K_L (L.mg^{-1})	16.079
	q_{max} (mg.g^{-1})	208.49
	R^2	0.831
Redlich-Petterson	K_F (mg.g^{-1}).(L.mg^{-1})$^{1/n}$	7952.713
	a	50.677
	b	0.890
	R^2	0.963
Toth	q_{max} (mg.g^{-1})	377.841
	K_T	3226.009
	n	0.198
	R^2	0.9998
Temkin	a (mg.g^{-1})	194.625
	b (g.mg^{-1})	0.0194
	R^2	0.322

Among the isotherm models tested, the Toth model provided the best fit (R^2 = 0.9998), indicating heterogeneous surface adsorption with a high maximum capacity (q_{max} = 377.84 mg·g^{-1}). The Redlich–Peterson model also provided a good fit (R^2 = 0.963), indicating hybrid adsorption behaviour. In contrast, the Langmuir model showed moderate agreement (R^2 = 0.831), while the Temkin model performed poorly (R^2 = 0.322). These results suggest that Fe^{3+} adsorption on modified oyster shell occurs on a heterogeneous surface with strong affinity and complex binding mechanisms.

Conclusion

This study shows that oyster shells that have been heat-treated and modified with H_3PO_4 are very good at removing Fe^{3+} ions from dirty water. The tests showed that the structure and chemistry of the oyster shells were successfully changed, leading to a larger surface area and the creation of phosphate groups. Adsorption experiments revealed rapid and efficient Fe^{3+} uptake, reaching nearly 100% removal within 120 minutes. Kinetic analysis showed that the main processes involved were chemisorption and pore diffusion, and the isotherm modeling pointed out that there were different types of interactions on the surface. The modified oyster shells, derived from abundant seafood waste, offer a sustainable and cost-effective solution for heavy metal remediation. These findings contribute to the development of environmentally friendly technologies for water treatment and support resource recovery through waste reuse.

Acknowledgments

This study was conducted at the laboratory of the Department of Chemistry and Environment, Joint Vietnam - Russia Tropical Science and Technology Research Center.

References

1. A. Solmaz, Ö.S. Bölükbaşi, Z.A. Sari, Environmental Science and Pollution Research 31 (2024) 19795-19814. https://doi.org/10.1007/s11356-024-32451-6
2. B. Roy, B. Bhunia, T.K. Bandyopadhyay, S.A. Khan, N.B. Nandi, P.C. Nath, Water pollution by heavy metals and their impact on human health, Wiley, 2024, p. 333-352.
3. A. Chernyaev, J. Zhang, S. Seisko, M. Louhi-Kultanen, M.J.S.R. Lundström, 13 (2023) 21445. https://doi.org/10.1038/s41598-023-48247-6
4. R. Lv, Y. Hu, Z. Jia, R. Li, X. Zhang, J. Liu, C. Fan, J. Feng, L. Zhang, Z. Wang, Hydrometallurgy 188 (2019) 194-200. https://doi.org/10.1016/j.hydromet.2019.07.005

5. L. Zhang, R. Bai, J. Zhang, Z. Chen, J. Guo, Environmental Research 274 (2025) 121284. https://doi.org/10.1016/j.envres.2025.121284
6. A. Middea, L.d.S. Spinelli, F.G. de Souza Junior, T.d.L.A.P. Fernandes, L.C. de Lima, V.M.T.S. Barthem, O.d.F.M. Gomes, R. Neumann, Mining 4 (2024) 37-57. https://doi.org/10.3390/mining4010004
7. D.A. Gkika, A.K. Tolkou, I.A. Katsoyiannis, G.Z. Kyzas, Separation and Purification Technology (2025) 132996. https://doi.org/10.1016/j.seppur.2025.132996
8. N. Nawar, M. Ebrahim, E. Sami, Academic Journal of Interdisciplinary Studies 2 (2013) 85-85. http://dx.doi.org/10.5901/ajis.2013.v2n6p85
9. Z. Zhou, Y. Wang, S. Sun, Y. Wang, L. Xu, Heliyon 8 (2022). https://doi.org/10.1016/j.heliyon.2022.e11938
10. W. Song, Y. Zeng, J. Wu, Q. Huang, R. Cui, D. Wang, Y. Zhang, M. Xie, D. Feng, Chemosphere 345 (2023) 140505. https://doi.org/10.1016/j.chemosphere.2023.140505
11. W.-T. Tsai, Materials 6 (2013) 3361-3372. https://doi.org/10.3390/ma6083361
12. M. Lu, X. Shi, Q. Feng, M. Zhang, Y. Guo, X. Dong, R. Guo, Journal of Environmental Chemical Engineering 9 (2021) 106708. https://doi.org/10.1016/j.jece.2021.106708
13. V. Veni, T. Brenda, Preparation of raw oyster shell for removal of coomassie brilliant blue R-250 dye from aqueous solution, IOP Conference Series: Earth and Environmental Science. IOP Publishing, 2021, p. 012039.
14. S. Rosli, M. Jameel, M. Mayzan, S. Shamsuddin, M. M-Raffi, A. Zainal, S.J.N.B. Saleem, Engineering, (2024). https://doi.org/10.26599/NBE.2024.9290074
15. L.M. Nguyen, N.T.T. Nguyen, T.T.T. Nguyen, T.T. Nguyen, D.T.C. Nguyen, T.V.J.E.C.L. Tran, 20 (2022) 1929-1963. https://doi.org/10.1007/s10311-022-01416-x
16. T.R. Sahoo, B. Prelot, Nanomaterials for the detection and removal of wastewater pollutants, Elsevier, 2020, p. 161-222.
17. C. Marchini, C. Triunfo, N. Greggio, S. Fermani, D. Montroni, A. Migliori, A. Gradone, S. Goffredo, G. Maoloni, J.J.C.G. Gómez Morales, Design, 24 (2023) 657-668. https://doi.org/10.1021/acs.cgd.3c01007